Experimental study of the boosters impact on the rocket aerodynamic characteristics

Andrzej Krzysiak
Department of Aerodynamic, Institute of Aviation, Lukasiewicz Research Network, Warszawa, Poland
Dawid Cieśliński
Department of Space Technology, Institute of Aviation, Łukasiewicz Research Network, Warsaw, Poland, and
Robert Placek and Pawel Kekus
Department of Aerodynamic, Institute of Aviation, Łukasiewicz Research Network, Warsaw, Poland

Abstract

Purpose – The purpose of this study is to determine the impact of two parallel boosters fixed to the ILR 33 AMBER 2 K core rocket stage on its aerodynamic characteristics in the subsonic and transonic regimes and for M = 2.3.

Design/methodology/approach – Wind tunnel tests of the rocket model were carried out in a trisonic wind tunnel using a six-component internal balance. Three rocket model configurations were investigated.

Findings – The results of the presented studies showed that the presence of boosters causes a significant increase in the total rocket drag, which depends on both the Mach number and the rocket flight phase. Experimental tests of the rocket model allowed to determine the difference in drag coefficient between active and passive flight versus Mach number. It was found that, in the case of a deviation from the rocket's flight direction, the aerodynamic coefficients strongly depend on the location of the boosters in relation to the direction of the deviation.

Practical implications – Studies of the rocket model aerodynamic characteristics allow the assessment of the influence of parallel boosters on rocket performance, which is important when the decision of a rocket staging type is taken.

Originality/value – The presented wind tunnel test results of the rocket model equipped with the two parallel boosters are an original contribution to the rocket research results presented in the literature.

Keywords Rockets, Parallel boosters, Wind tunnel tests, Aerodynamic characteristics

Paper type Research paper

Nomenclature

C = chord (m);
Cd = drag coefficient;
C_l = lift coefficient;
C_m = pitching moment coefficient;
B = booster;
M = Mach number;
R = core rocket unit;
Re = Reynolds number;
α = angle of attack; and
γ = roll angle.

Symbols, definitions, acronyms and abbreviations

CAD = Computer aided design;
CFD = Computational fluid dynamics;
GNC = Guidance, navigation, control;
NATO = North Atlantic Treaty Organisation;
SLS = Space Launch System;
SRB = Solid rocket booster; and
The USA = The United States of America.

Introduction

Through decades of rocket development, the pursuit of performance improvement accompanied constructors and scientists. Until the twentieth century, most of the rockets were single-stage constructions. However, it should be noted that the first concepts of multistage projectiles had been introduced by a Polish–Lithuanian pioneer Siemienowicz in the seventeenth century. The theoretical consideration led by Tsiolkovsky (Suresh and Sivan, 2015), resulting in the classical rocket equation, confirmed that a multistage rocket is necessary for space travel. The ability of a rocket to reach higher or further targets can be expressed by the delta-v budget (a direct result of the rocket equation), and on this basis, it is clearly seen that vehicle staging is the best feasible way to obtain performance improvements without the need for a technology breakthrough in propulsion.

The current issue and full text archive of this journal is available on Emerald Insight at: **https://www.emerald.com/insight/1748-8842.htm**

Aircraft Engineering and Aerospace Technology
 [ISSN 1748-8842]
[DOI 10.1108/AEAT-01-2022-0025]

The authors thank Paweł Ruchała for his contributions to the wind tunnel campaign presented in this article.

Received 2 February 2022
Revised 4 May 2022
Accepted 18 June 2022

Staging can be realised in two ways: parallel or series propulsion stages (Turner, 2006; Suresh and Sivan, 2015), as presented in Figure 1. In parallel staging, boosters that work simultaneously with core stages are often called stage "zero". For launchers (vehicles that enable one to achieve space orbits), adding parallel staging aims to increase their capacity for specific destinations. It improves vehicle versatility without major interference in the baseline design {see Falcon 9 vs Falcon Heavy [Space Exploration Technologies (SpaceX), 2020] outlines or Ariane 6 configurations with two or four boosters (Arianespace, 2018)}. If series staging was applied instead, then some serious implications caused by the additional elongation would be introduced to the vehicle (increased vehicle length influences dynamic characteristics and susceptibility to vibrations and increases bending loads). On the other hand, parallel staging brings other technical inconveniences compared to the series solution, for example, a pressure drag increase because of the presence of additional off-the-core bodies, while the boosters are attached during the launch phase through a dense atmosphere. Furthermore, any misalignment or difference in performance between each of the boosters results in a non-axial thrust force application, so additional control manoeuvres for maintaining the nominal trajectory are required, causing at least slight performance losses. During stage separation (after burnout), serial stages do not cause a risk of collision with the upper stages, unlike parallel boosters, which require additional analyses for the booster jettisoning process.

Many launchers over the world use parallel boosters, from the first ever Soviet launcher (R-7) (van Riper, 2004), Soyuz, Proton, Japanese H-II, European Ariane 4, 5 and Ariane 6 vehicles, Indian GSLV (Suresh, 2008) or the US family of launchers represented by Atlas, Delta IV, the Space Shuttle (Suresh and Sivan, 2015), Falcon Heavy and the Space Launch System (SLS) (NASA, 2018). However, it is not an exhaustive list of launchers that use boosters, neither among the countries nor over time (Turner, 2006).

Figure 1 Methods for rockets staging

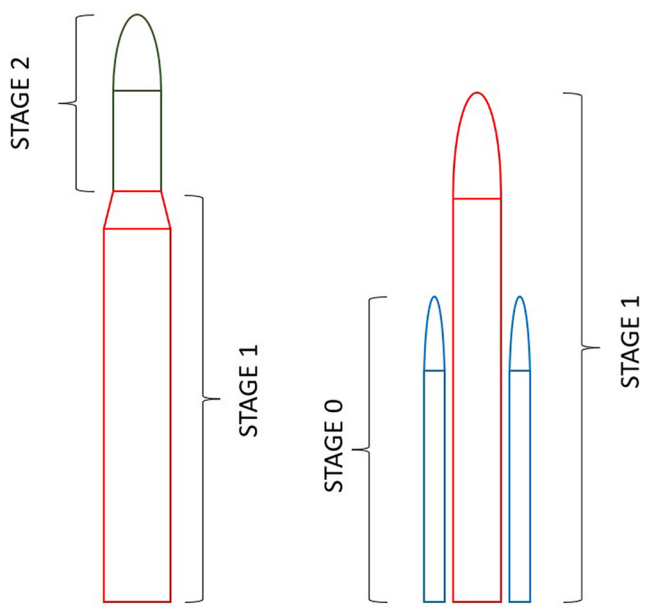

Note: Serial (left) and parallel (right)

Among suborbital rockets (capable of reaching outer space altitudes but unable to perform any orbital revolution), boosters are not as popular as among launchers, mostly because of the above-mentioned need for prevention of performance misalignment. However, if introduced to sounding rockets or missiles, boosters are used to not only increase capacity (performance) but also decrease rocket susceptibility to launch conditions (increase launch velocity during lift-off). The examples of sounding rockets or missiles with boosters are: Rheintochter R3, Meteor rockets, S-200 (SA-5 in NATO code), Bloodhound, Otomat and Seaslug (Taylor, 1980). This article concerns the ILR-33 Amber 2 K sounding rocket, where parallel staging was applied. For the purpose of this paper, the name *booster* refers to an additional strap-on propulsion stage ("Stage 0").

Polish rockets with boosters

Although they did not have any orbital launchers, Polish scientists and engineers participated in rocket- or space-related technologies since their very beginning. In 1850s, Łukasiewicz distilled kerosene from oil (Mierzecki, 2014). In the 1880s, Polish scientists Olszewski and Wróblewski were the first to liquefy, for example, oxygen (Wróblewski and Olszewski, 1883) or hydrogen (Wróblewski and Olszewski, 1884). These media are popular propellants in launch vehicles to this day.

Meteor rocket program

From 1958 to 1974, 12 types of sounding rockets made more than 327 flights. A rocket family named Meteor, designed by Łukasiewicz – Institute of Aviation, proved most successful and allowed to run a seven-year long atmosphere sounding program. High-altitude launches took place at the Łeba Rocket Sounding Station, located in a former German rocket test base (Wolański and Wiśniowski, 2014). After the Meteor program, the development of rocket technologies in Poland was postponed for nearly 40 years.

ILR-33 AMBER sounding rocket

The ILR-33 AMBER rocket is a suborbital platform developed by Łukasiewicz – Institute of Aviation. There are some similarities between METEOR and ILR-33, such as using parallel staging or their maximum apogee of approximately 100 km. However, METEOR used only solid propulsion systems; ILR-33 uses a main-hybrid motor with polyethylene as fuel and high-test peroxide as oxidiser, fitting in with global trends in modern chemical propulsion systems. Two solid strap-on boosters are used during the first flight phase (Marciniak *et al.*, 2018). The rocket can be used in atmosphere sounding, microgravity research, astronomy missions and technology validation. Between 2017 and 2019, there were three flights with apogees in the range of 11–23 km (Pakosz *et al.*, 2020). The first version of the rocket was able to reach altitudes of about 60 km. As the aim of the rocket is to offer flights for test and technology block maturation in microgravity and space environment (10 kg to 100 km), its performance was enhanced by improving the solid rocket boosters.

Figure 2 ILR-33 with smaller boosters (left); ILR-33 2 K with improved SRB (right)

Sources: Leszek Loroch (left); Pakosz *et al*., 2020 (right)

ILR-33 AMBER 2 K

The ILR-33 AMBER 2 K rocket is a development version of the AMBER platform with new boosters. It reaches apogees of over 100 km with payloads of 10 kg (Figure 2).

Aerodynamic design

The non-standard shape of the rocket required a wind tunnel investigation of the first version of ILR - 33 (Ruchała *et al.*, 2017). To optimise the size of the SRBs, a parametric model was used to generate configurations varying in diameters, total masses and impulses (Pakosz *et al.*, 2020).

Separation of the boosters should occur immediately after their burnout. To accelerate this process, the shape of the booster head and its orientation with respect to the core body of the rocket were investigated. Two different shapes were investigated: smooth (semi-parabolic) and sharp (truncated cylinder). The computational fluid dynamics (CFD) investigation showed that the sharp one promotes separation several times faster than the smooth one (with a negligible drag increase, as the Mach number at booster separation was below 0.8). That comparison was made for the first version of the ILR-33 (Nowakowski *et al.*, 2017). It should be noted here that, once validated (by experimental results), CFD methods are invaluable in the analyses of various modifications to the rocket configuration (including attached bodies, such as the boosters), and in many cases, they can replace experimental research. The use of CFD for rockets aerodynamic characteristic was widely described in the literature (Lopez *et al.*, 2013; Luedeke and Calvo, 2009; Rasuo *et al.*, 2015; Rogers *et al.*, 2015).

The new ILR-33 boosters have an increased diameter (0.176 m instead of 0.1 m) and length. Booster separation now occurs at Mach approximately 2.3, so drag will play a more significant role compared to the first version. Furthermore, the smooth shape was chosen because of system engineering (an additional volume was required in the booster head, which advantages the smooth version). In the first approach, the orientation of the heads with respect to the core body was to remain the same as in the ILR-33 (version 1) – with the cylinder generatrix away from the core. This orientation encourages automatic booster separation from the rocket because of pressure distribution (lifting body shape). However, technological issues (booster joint location) forced rotating of the orientation to such, where the cylinder generatrix is close to the core (this is the final configuration tested in the wind tunnel; Figure 3). No axisymmetric heads were considered.

An early version of the ILR-33 Amber rocket, which is not the subject of this article, was previously tested under subsonic conditions in the open-jet low-speed wind tunnel at Łukasiewicz – Institute of Aviation, where the influence of fins and boosters on axial and normal forces and moments was investigated with the aim of further optimising the design (Ruchała *et al.*, 2017). Other recent examples of subsonic rocket testing include evaluating the impact of thrust vectoring lateral jets on the aerodynamic characteristics of a missile (Ocokolić and Rašuo, 2012), iterative shape optimisation of missile wings (Ocokolić *et al.*, 2017) and an investigation of the impact of nozzle configurations in the near wake of a generic rocket (Wolf *et al.*, 2012). Supersonic tests have recently been used for an evaluation of booster characteristics of the SLS during separation using laser sheet visualisation (Danehy *et al.*, 2019), as well as for determining aeroacoustic performance of modern launchers – VEGA (Imperatore *et al.*, 2005; Camussi *et al.*, 2020) and the SLS (Garbeff *et al.*, 2019; Roozeboom *et al.*, 2019; Steva *et al.*, 2019) using a wide variety of techniques, including pressure-sensitive paint, steady and unsteady pressure sensors, shadowgraph and schlieren photography.

Research methodology of the wind tunnel tests

The experimental tests of the ILR-33 2 K Amber rocket model were conducted in a blow-down type, trisonic N-3 wind tunnel with partial recirculation of the flow, equipped with a 0.6 m × 0.6 m test section. Wind tunnel tests were carried out both at sub- and transonic Mach numbers, M = 0.3–1.1, and at a supersonic one, M = 2.3. At subsonic and transonic Mach regimes, the lower and upper walls of the test section were perforated (side walls were solid). For supersonic tests, all walls of the wind tunnel test section were solid.

Measurements of the aerodynamic characteristics of the rocket mode were performed using a six-component strain gauge balance FFA I-646–2. The balance had the additional functionality of measuring static pressure in the middle of its length. The basic dimensions of the model are presented in Figure 3. The rocket model was equipped with four fins (permanently) and removable boosters. The core unit of the model was made of steel and the booster bodies were made of aluminium. A detailed description of the ILR-33 2 K model was presented by Pakosz *et al.* (2020). During the experimental campaign, the ILR-33 2 K Amber rocket model was tested at three different roll angles (in relation to the angle of attack plane; Figure 3), that is, $\gamma = 0°$, 45° and 90°. The boosters were mounted only at $\gamma = 0°$ and 90°.

Before the test campaign, balance and sting deflections caused by the normal force and the pitching moment, as well as by the sweep angle of the flow, were determined and implemented to test data corrections. The aerodynamic coefficients were determined by dividing the measured values of the aerodynamic forces and moments by reference area (cross-sectional area of the model core unit – 0.00062 m^2), by the reference length (diameter of the model core unit –

Figure 3 Dimensions and configurations of the ILR-33 2 K Amber rocket model including, definition of roll angle

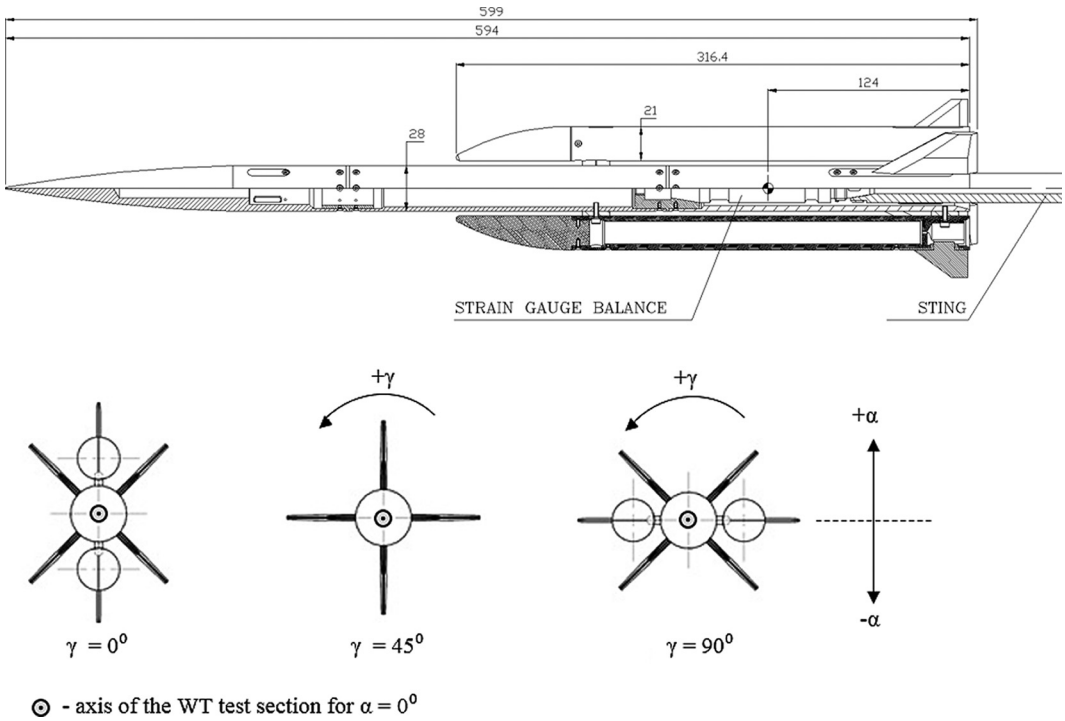

0.028 m) and by the dynamic pressure value. Furthermore, separate measurements of bottom pressure, that is the pressure acting on the bottom of the rocket core unit and boosters, were carried out in a range of Mach numbers (M = 0.4 ÷ 1.1) using a specially prepared twin model. The twin rocket model had the same dimensions as the main model and was fixed to test section walls using cables (at a zero angle of attack), without the sting that normally holds the model, as shown in Figure 4. The bottom pressure values of the boosters were used for the total drag calculation in the active flight case, whereas the core unit bottom pressure was used for the total drag calculation in the passive flight case. The influence of the angle of attack on the bottom pressure of the boosters was neglected.

Measurement uncertainty

The uncertainty of the measurements presented in this article was established using datum measurements taken throughout the campaign. The datum was set at zero angle of attack of the rocket relative to the flow and was taken at the beginning, in the middle and at the end of each run. The three datums were used to calculate two deltas, that is, changes in forces and moments exerted on the rocket from the beginning to the middle and from the middle to the end of a run. These deltas represent typical deviations of loading for a particular configuration during a run and are a more realistic indicator of measurement uncertainty than that estimated using linear error propagation, which was found to severely overestimate uncertainty.

To obtain uncertainty values for each force and moment coefficient, the standard deviation was calculated of both deltas from each of the approximately 80 runs (yielding more than 160 samples) and multiplied by 1.96 to obtain the 95% confidence interval. Finally, the uncertainty of the bottom pressure measurements was added for the drag coefficient. The resulting uncertainties for drag, lift and pitching moment coefficients are 0.049, 0.047 and 0.32, respectively.

Figure 4 ILR-33 2 K Amber rocket model and twin model in the N-3 wind tunnel

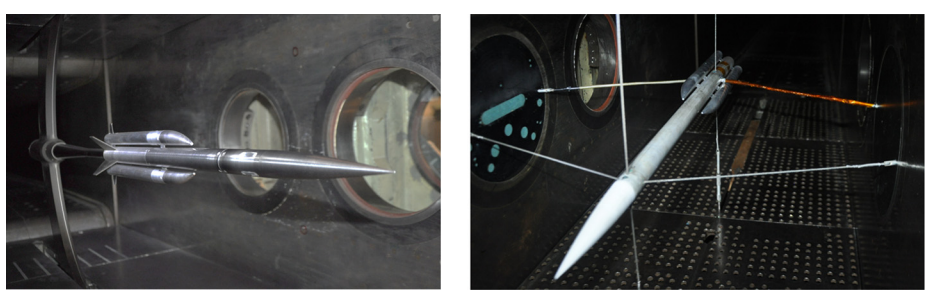

Examples of test results

The primary issue considered in the course of research on the ILR-33 AMBER 2 K rocket model in the N-3 trisonic wind tunnel was the influence of two parallel boosters on the aerodynamic characteristics of the rocket. Wind tunnel tests were performed for various model configurations (Figure 4) in the range of Mach numbers M = 0.4 ÷ 1.1 and also for M = 2.3. Furthermore, for each of the tested model configurations, the aerodynamic characteristics of the rocket in active flight (with rocket engines operating) and passive flight (with engines inoperative) were considered. The aerodynamic characteristics of the rocket in the active phase were determined by introducing appropriate corrections that used the bottom pressure measured using the rocket twin model.

In Figure 5, the difference of the drag coefficient value between the active and passive flight (bottom drag) of the core rocket unit (without boosters), equipped only with fins (configuration $\gamma = 45^{\circ}$; Figure 3), versus Mach number for $\alpha = 0°$ is presented. Because of the lack of measurements in the range of Mach numbers greater than M = 1.1 and smaller than M = 2.3, the relationship ΔCd = f(M) in this range was estimated based on the results of research taken from the literature (Suttles, 1964) (dotted line).

The bottom drag of the main rocket unit is significant (25%–35% of the drag of the main rocket unit) and reaches the maximum value of ΔCd approximately 0.3 at M = 1.1.

In Figure 6, the impact of the boosters on the total drag coefficient of the rocket in the case of flight with the boosters in the active or passive phase is presented for the subsonic and transonic Mach numbers and for $\alpha = 0^{\circ}$. For the passive flight phase in the range of Mach numbers greater than M = 1.1 and smaller than M = 2.3, the relationship ΔCd = f(M) was estimated based on the literature (Suttles, 1964) (dotted line). For the supersonic Mach number M = 2.3 during the active flight phase, it was impossible to determine the value of the rocket total drag coefficient, because the twin rocket model was not tested at this Mach number.

The presence of boosters causes a significant increase in the total rocket drag, which depends both on the Mach number and on the rocket flight phase (boosters active or passive). In the range of Mach numbers M = 0.4 ÷ 1.0, the additional rocket drag, associated with the presence of boosters, grows approximately exponentially with the

Figure 5 The bottom drag coefficient of the core rocket unit versus the Mach number

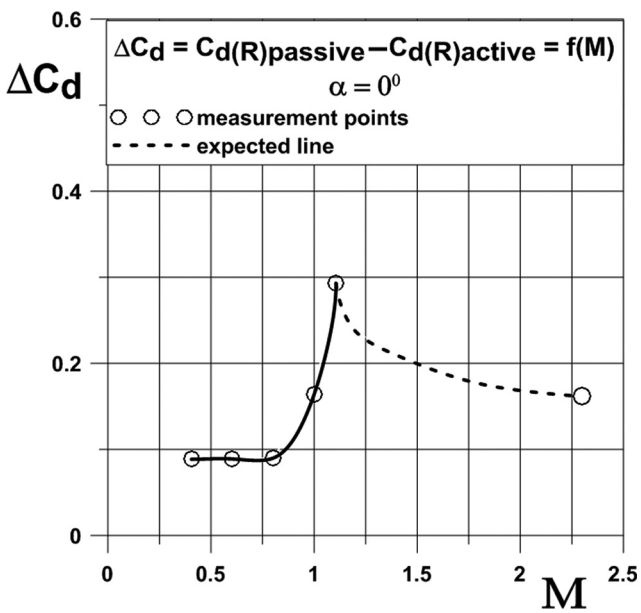

Figure 6 Impact of boosters on the total drag coefficient of the rocket

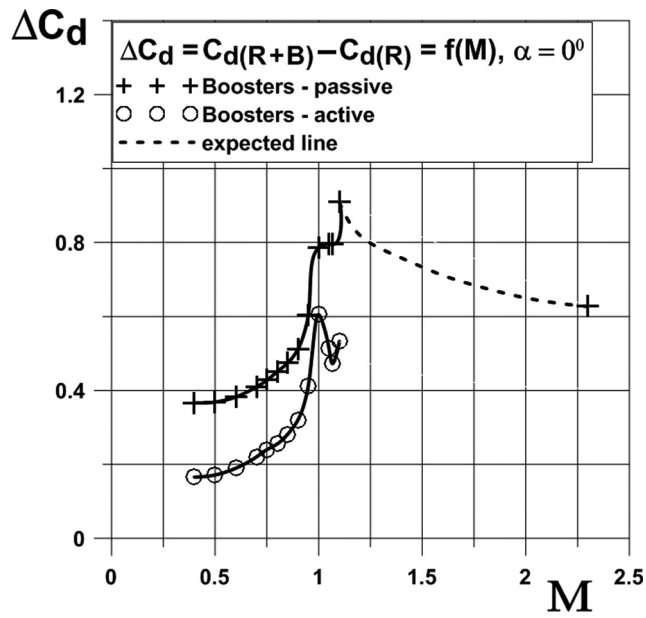

Figure 7 Impact of the location of the boosters on rocket drag versus angle of attack

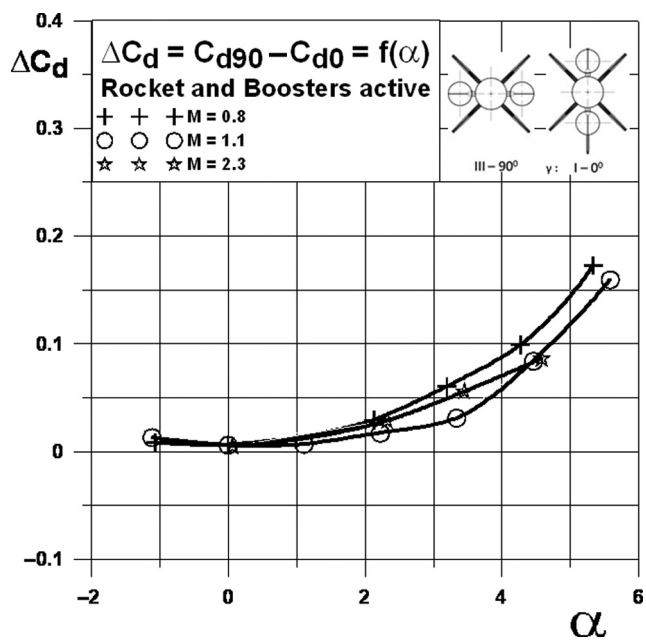

Figure 8 Impact of the location of the boosters on the rocket lift and pitching moment versus angle of attack

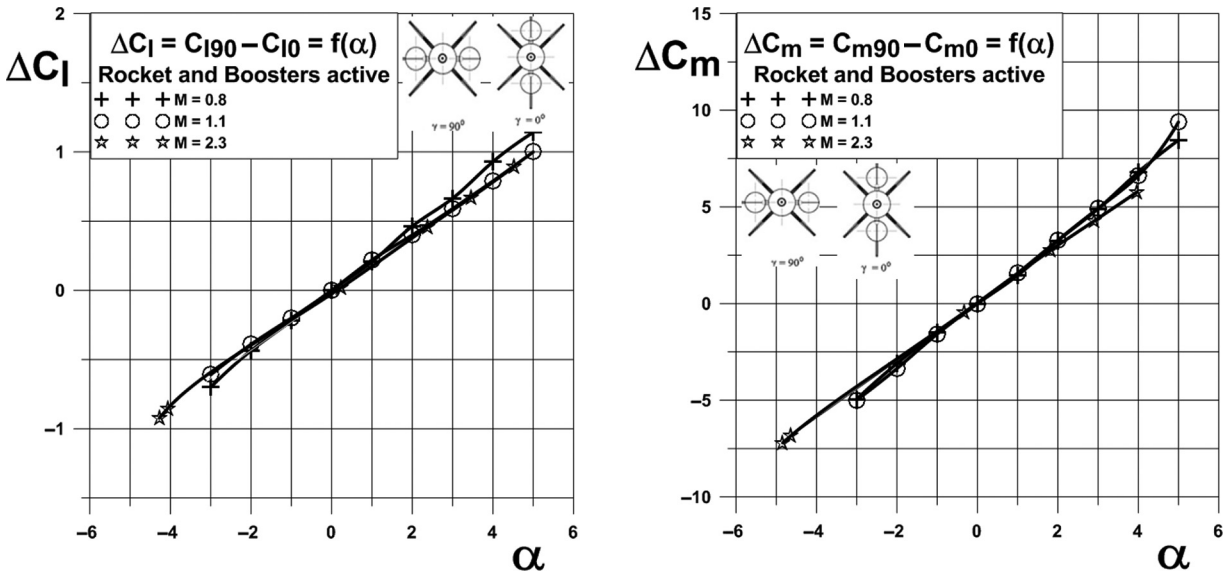

increasing Mach number, from ΔCd = 0.17 at M = 0.4 to ΔCd = 0.6 at M = 1.0 with active boosters and from ΔCd = 0.37 at M = 0.4 to ΔCd = 0.79 at M = 1.0 with inactive boosters. In the range of transonic Mach numbers M = 1.0 ÷ 1.1, the additional rocket drag because of the presence of active boosters first decreases with increasing Mach number, and then it grows. In the case of inactive boosters for Mach numbers in the range M = 1.0 ÷ 1.1, the additional rocket drag keeps an approximately constant value in the range M = 1.0 ÷ 1.08 and rapidly increases with the increasing Mach number. It can be assumed that the changes in drag coefficient in the range of Mach numbers M = 1.0 ÷ 1.1 are related to the appearance of a shock system in the surroundings of the boosters, but this issue has not been investigated.

As expected, the increase in Mach number from M = 1.1 up to M = 2.3 causes a decrease in additional rocket drag associated with the presence of boosters from ΔCd = 0.91 at M = 1.1 to ΔCd = 0.62 at M = 2.3 for rocket flight with the boosters inactive.

In Figure 7, the impact of the location of the boosters in relation to the angle of attack plane (boosters located in the pitching plane $\gamma = 0°$ or in the yawing plane $\gamma = 90°$; Figure 3) on the rocket drag versus the angle of attack for Mach numbers M = 0.8, 1.1 and 2.3 is presented.

As can be seen, the Mach number value has a relatively small effect on the characteristic ΔCd = f(α) presented in Figure 7.

In Figure 8, the impact of the location of the boosters in relation to the angle of attack plane on the rocket lift and the pitching moment coefficients versus the angle of attack for Mach numbers M = 0.8, 1.1 and 2.3 is presented. The differences in the lift and pitching moment coefficients between the configuration at the roll angle $\gamma = 90°$ in comparison with $\gamma = 0°$ rise approximately linearly with increasing angle of attack. The value of the Mach number has a relatively small effect on the characteristics $\Delta C_l = f(\alpha)$ and $\Delta C_m = f(\alpha)$ as presented in Figure 8.

Conclusions

Experimental measurements of aerodynamic characteristics of the ILR-33 AMBER 2 K rocket model equipped with two parallel boosters in the trisonic wind tunnel N-3 were performed. Wind tunnel tests were carried out at Mach numbers in the range M = 0.4 ÷ 1.1 and for M = 2.3. Based on the test results, the influence of the boosters during their active phase (with rocket engines operating) and passive flight (with engines inoperative) on rocket drag, lift and pitching moment coefficient is presented. The results showed that:

- The bottom drag of the main rocket unit increases in the subsonic and transonic regimes with the increasing Mach number and reaches the maximum value of ΔCd approximately 0.3 at M = 1.1. For Mach numbers higher than M = 1.1, the bottom drag of the rocket decreases and has a value of ΔCd approximately 0.16 at M = 2.3.
- The presence of boosters causes a significant increase of the total rocket drag (30%–50%), which depends both on the Mach number and on the rocket flight phase (boosters active or passive). In the subsonic and transonic regimes (M = 0.4 ÷ 1.0), the presence of boosters causes an approximately exponential drag increase with the increasing Mach number. This drag increase caused by the presence of the booster reaches a maximum value of ΔCd = 0.6 at M = 1.0 in the active booster case and ΔCd = 0.91 at M = 1.1 with inactive boosters.
- In the case of a deviation from the rocket's flight direction (sideslip), the aerodynamic coefficients strongly depend on the location of the boosters in relation to the direction of the deviation. Drag, lift and pitching moment coefficients versus the angle of attack were found to have a significantly higher value when the rocket deflection plane is perpendicular to the plane of the boosters (Configuration III – 90°) in comparison with the parallel direction (Configuration I – 0°).

References

Arianespace (2018), "Ariane 6 user's manual. Issue 1. Revision 0", chapter 5-2, p. 89.

Camussi, R., Di Marco, A., Stoica, C., Bernardini, M., Stella, F., De Gregorio, F., Paglia, F., Romano, L. and Barbagallo, D. (2020), "Wind tunnel measurements of the surface pressure fluctuations on the new VEGA-C space launcher", *Aerospace Science and Technology*, Vol. 99, p. 105772.

Danehy, P.M., Wisser, B.M., Fahringer, T.W., Winski, C.S., Falman, B.E., Shea, S., Boyda, M. and Lowe, K.T. (2019), "Laser light sheet flow visualization of the space launch system booster separation test", AIAA paper 2019-3507, paper presented at the AIAA Aviation 2019 Forum, 17-21 June, Dallas, TX.

Garbeff, T.J. II., Baerny, J.K. and Ross, J.C. (2019), "Wind tunnel flow field visualizations of the space launch system vehicle ascent", AIAA paper 2019-3299, paper presented at the AIAA Aviation 2019 Forum, 17-21 June, Dallas, TX.

Imperatore, B., Guj, G., Ragni, A., Pizzicaroli, A. and Giulietti, E. (2005), "Aeroacoustic of the VEGA launcher wind tunnel tests and full scale extrapolations", AIAA paper 2005-2913, paper presented at the 11th AIAA/CEAS Aeroacoustics Conference, 23-25 May 2005, Monterey, CA.

Lopez, D., Domınguez, D. and Gonzalo, J. (2013), "Impact of turbulence modelling on external supersonic flow field simulations in rocket aerodynamics", *International Journal of Computational Fluid Dynamics*, Vol. 27 Nos 8/10, pp. 332-341, doi: 10.1080/10618562.2013.867951.

Luedeke, H. and Calvo, J.B. (2009), "A fluid structure coupling of the ariane-5 during start phase by DES", *Proceedings of 6th European Symposium on Aerothermodynamics for Space Vehicles*, 3-6 November 2008, *Versailles*.

Marciniak, B., Okninski, A., Bartkowiak, B., Pakosz, M., Sobczak, K., Florczuk, W., Kaniewski, D., Matyszewski, J., Nowakowski, P., Cieslinski, D. and Rarata, G. (2018), "Development of the ILR-33 'amber' sounding rocket for microgravity experimentation", *Aerospace Science and Technology*, Vol. 73, pp. 19-31, doi: 10.1016/j.ast.2017.11.034.

Mierzecki, R. (2014), "Chemical ideas and the development of chemical and petroleum industry on the polish territory since 1850 to 1920", Technical Transactions. Fundamental Sciences, Publishers of the Cracow University of Technology, 1-NP/2014.

NASA (2018), "Space launch system (SLS) mission planner's guide", pp. 13. revision A, National Aeronautics and Space Administration (NASA), Document No: ESD 30000

Nowakowski, P., Okninski, A., Pakosz, M., Cieslinski, D., Bartkowiak, B. and Wolanski, P. (2017), "Development of small solid rocket boosters for the ILR-33 sounding rocket", *Acta Astronautica*, Vol. 138, pp. 374-383, doi: 10.1016/j.actaastro.2017.06.007.

Ocokolić, G. and Rašuo, B. (2012), "Testing an anti-tank missile model with jet simulation in the T-35 subsonic wind tunnel", *Scientific Technical Review*, Vol. 62 Nos 3/4, pp. 14-20.

Ocokolić, G., Rašuo, B. and Bengin, Č. (2017), "Aerodynamic shape optimization of guided missile based on wind tunnel testing and computational fluid dynamics simulation", *Thermal Science*, Vol. 21 No. 3, pp. 1543-1554.

Pakosz, M., Majewska, E., Matysek, K., Noga, T., Nowakowski, P. and Ptasinski, G. (2020), "Design modifications for performance enhancement of a suborbital rocket ILR-33 AMBER 2K", IAC-20-D2.6.7, paper presented at the 71st International Astronautical Congress (IAC) – The Cyber Space Edition, International Astronautical Federation (IAF), 12-14 October 2020.

Rogers, S.E., Dalle, D.E. and Chan, W.M. (2015), "CFD simulations of the space launch system ascent aerodynamics and booster separation", *Proceedings of 53rd AIAA Aerospace Sciences Meeting*, 5-9 January 2015, *Kissimmee, FL*, doi: 10.2514/6.2015-0778.

Roozeboom, N.H., Powell, J., Baerny, J.K., Murakami, D.D., Ngo, C.L., Garbeff, T.J., Ross, J.C. and Flach, R. (2019), "Development of unsteady pressure-sensitive paint application on NASA space launch system", AIAA paper 2019-3502, paper presented at the AIAA Aviation 2019 Forum, 17-21 June, Dallas, TX.

Ruchała, P., Placek, R., Stryczniewicz, W., Matyszewski, J., Cieśliński, D. and Bartkowiak, B. (2017), "Wind tunnel tests of influence of boosters and fins on aerodynamic characteristics of the experimental rocket platform", *Transactions on Aerospace Research*, Vol. 2017 No. 4, pp. 82-102.

Space Exploration Technologies (SpaceX) (2020), "Falcon user's guide", pp. 2. April 2020

Steva, T.B., Pollard, V.J. and Herron, A.J. (2019), "Space launch system aeroacoustic wind tunnel test results", AIAA paper 2019-3303, paper presented at the AIAA Aviation 2019 Forum, 17-21 June, Dallas, TX.

Suresh, B.N. (2008), "History of Indian launchers", *Acta Astronautica*, Vol. 63 Nos 1/4, pp. 428-434, doi: 10.1016/j.actaastro.2007.12.066.

Suresh, B.N. and Sivan, K. (2015), *Integrated Design for Space Transportation System*, Springer India, New Delhi, pp. 142-143, doi: 10.1007/978-81-322-2532-4.

Suttles, J.T. (1964), "Aerodynamic characteristics from Mach 0.22 to 4.65 of a two-stage rocket vehicle having an unusual nose shape", NASA TN D-2163.

Taylor, M.J.H. (1980), *Missiles of the World*, Ian Allan.

Turner, M. (2006), *Rocket and Spacecraft Propulsion. Principles, Practice and New Developments*, 2nd ed., Springer – Praxis Books in Astronautical Engineering, Chichester.

Van Riper, A. (2004), *Rockets and Missiles; the Life Story of a Technology*, Grenwood Press, London, p. 77.

Wolański, P. and Wiśniowski, W. (2014), "Institute of aviation activities in the field of space research", *Transactions of Institute of Aviation*, Vol. 1 No. 234, pp. 9-16. Scientific Publishers of the Institute of Aviation, Warsaw, Poland.

Wolf, C.C., Klei, C.E., Buffo, R.M., Hörnschemeyer, R. and Stumpf, E. (2012), "Comparison of rocket near-wakes with and without nozzle simulation in subsonic freestream conditions", AIAA paper 2012-3019, paper presented at the 42nd AIAA Fluid Dynamics Conference and Exhibit, 25-26 June, New Orleans, LA.

Wróblewski, Z.F. and Olszewski, K. (1883), "Über die verflüssigung des sauerstoffs, stickstoffs imd kohlenoxyds", *Annalen der Physik und Chemie*.

Further reading

Rasuo, B. and Bengin, A. (2017), "Aerodynamic shape optimization of guided missile based on wind tunnel testing and CFD simulation", *Thermal Science*, Vol. 21 No. 3, pp. 1543-1554, doi: 10.2298/TSCI150515184O.

Wróblewski, Z.F. (1884), "Sur la liquéfaction de l'hydrogène", *Comptes Rendus*, Vol. 98 No. 5, pp. 304-305.

Corresponding author

Andrzej Krzysiak can be contacted at: andrzej.krzysiak@ilot.edu.pl